

Brane Tilings, M2-branes and Chern-Simons Theories

JOHN DAVEY, AMIHAY HANANY, NOPPADOL MEKAREEYA AND
GIUSEPPE TORRI

Theoretical Physics Group, The Blackett Laboratory
Imperial College London, Prince Consort Road
London, SW7 2AZ, UK

j.davey07, a.hanany, n.mekareeya07, giuseppe.torri08@imperial.ac.uk

We investigate $(2 + 1)$ -dimensional quiver Chern-Simons theories that arise from the study of M2-branes probing toric Calabi-Yau 4-folds. These theories can be elegantly described using brane tilings. We present several theories that admit a tiling description and give details of these theories including the toric data of their mesonic moduli space and the structure of both their Master space and baryonic moduli space. Where different toric phases are known, we exhibit the equivalence between the vacua. We identify some of the mesonic moduli spaces as cones over smooth toric Fano 3-folds.

1. Introduction

Recently, there has been substantial progress in understanding M-theory on various different backgrounds. In particular M-theory on backgrounds of $\text{AdS}_4 \times X^7$, where X^7 is a Sasaki-Einstein 7-manifold, has been studied in great detail. These geometries are believed to correspond to world-volume theories of M2-branes that probe Calabi-Yau 4-fold singularities [1, 2, 3, 4]. These singularities can be identified with the cone over the aforementioned Sasaki-Einstein manifolds.

When M2-branes probe a Calabi-Yau 4-fold that admits a toric description, the branes' world-volume is thought to be well described by a $\mathcal{N} = 2$ $(2+1)$ -dimensional quiver Chern-Simons (CS) theory [3, 4, 5, 6, 7] which can be elegantly represented by a *brane tiling* [4, 8, 9, 10, 12]. This brane tiling technology was originally developed to understand the $(3 + 1)$ -dimensional gauge theories that describe D3-branes probing toric Calabi-Yau (CY) 3-fold singularities [13, 14], [12, 15, 16], [17, 18]. It is convenient and perhaps

not too surprising [4, 8] that the tilings used to describe M2-brane theories have many features in common with the original D3-brane tilings. Brane tilings have proven to be an incredibly powerful tool for studying a number of interesting phenomena, for example transitions between different singularities using the *Higgs mechanism* [10, 11] and also *toric duality* [6, 9, 19].

In this paper, we summarize an exploration of a class of gauge theories that arise from the study of M2-branes probing CY 4-folds which are cones over smooth toric *Fano 3-folds* [20]. These Fano 3-folds are 3 dimensional complex manifolds admitting positive curvature. It is known that there are precisely 18 of these surfaces [20, 21, 22]. It is thought that the investigation of Fano 3-folds may be as fruitful as the recent intensive study of their 2 dimensional analogues (the del Pezzo surfaces) [23, 24, 25] [14].

2. The $\mathcal{N} = 2$ supersymmetric CS theories in $(2 + 1)$ dimensions

In this paper we consider brane tilings that correspond to $(2 + 1)$ -dimensional $\mathcal{N} = 2$ supersymmetric CS theories. Each theory admits a $U(N)^G$ gauge symmetry, has matter fields that transform in bi-fundamental and adjoint representations, and has specific set of interactions. The Lagrangian for such a theory can be written in $\mathcal{N} = 2$ superspace notation as

$$\mathcal{L} = - \int d^4\theta \left(\sum_{X_{ab}} X_{ab}^\dagger e^{-V_a} X_{ab} e^{V_b} - i \sum_{a=1}^G k_a \int_0^1 dt V_a \bar{\mathcal{D}}^\alpha (e^{tV_a} \mathcal{D}_\alpha e^{-tV_a}) \right) + \int d^2\theta W(X_{ab}) + \text{c.c.} , \quad (2.1)$$

where a indexes the gauge groups ($a = 1, \dots, G$) and X_{ab} are bi-fundamental chiral superfields, accordingly charged. V_a are the vector multiplets, \mathcal{D} is the superspace derivative, W is the superpotential and k_a are the CS levels, which are integer valued. An overall trace is implicitly taken since all of the fields are matrix-valued. Each chiral superfield appears exactly twice in the superpotential - once in a positive term and once in a negative term. This is known as the *toric condition* on the superpotential [26].

The vacuum equations are given by

$$\partial_{X_{ab}} W = 0 , \quad (2.2)$$

$$\mu_a(X) := \sum_{b=1}^G X_{ab} X_{ab}^\dagger - \sum_{c=1}^G X_{ca}^\dagger X_{ca} + [X_{aa}, X_{aa}^\dagger] = 4k_a \sigma_a , \quad (2.3)$$

$$\sigma_a X_{ab} - X_{ab} \sigma_b = 0 . \quad (2.4)$$

The first set of equations (2.2) are the *F-term equations*, whose space of solutions is called the *Master space* [27]. The others - (2.3) and (2.4) are called the *D-term equations* in analogy to the vacuum equations of $\mathcal{N} = 1$ gauge theories in $(3 + 1)$ dimensions, with the last equation (2.4) being a new addition.

It should be noted that, in the absence of CS terms, this theory can be viewed as a dimensional reduction of a $(3 + 1)$ -dimensional $\mathcal{N} = 1$ supersymmetric theory. In particular, σ_a , the real scalar in the vector multiplet, arises from the zero mode of the component of the vector field in the reduced direction. We refer to the space of all solutions of (2.2), (2.3) and (2.4) as the *mesonic moduli space*, and denote it as \mathcal{M}^{mes} .

It can be shown that

$$\sum_a k_a = 0 \tag{2.5}$$

is a necessary condition for the moduli space to have a branch which is a Calabi–Yau four-fold [3, 4, 5]. This branch can be interpreted as the space transverse to the M2-branes.

Let us consider the abelian case¹ in which the gauge group is $U(1)^G$. We consider the branch in which all of the bi-fundamental fields are generically non-zero. In this case, the solutions to the first set of equations (2.2) give the *irreducible component* of the Master space, $\text{Irr}\mathcal{F}^b$ [27].

The third equation (2.4) sets all σ_a to a single field, let's say σ .

The second set of equations in (2.3) consists of G equations. The sum of all of these equations is identically zero, and so there are actually only $G - 1$ linearly independent equations. These $G - 1$ equations can be divided into one along the direction of the vector k_a , and $G - 2$ perpendicular to the vector k_a . The former fixes the value of σ and leaves a \mathbb{Z}_k action, where $k \equiv \text{gcd}(\{k_a\})$, by which we need to quotient out in order to obtain the mesonic moduli space. The remaining $G - 2$ equations can be imposed by the symplectic quotient of $U(1)^{G-2}$. Thus, the mesonic moduli space can be written as

$$\mathcal{M}^{\text{mes}} = \text{Irr}\mathcal{F}^b // (U(1)^{G-2} \times \mathbb{Z}_k) . \tag{2.6}$$

The reader should note that these $G - 2$ directions correspond to *baryonic charges* that arise from D-terms although the *total* number of baryonic charges is four less than the number of external points of the toric diagram [9].

¹ The mesonic moduli space of the non-abelian $U(N)^G$ theory is expected to be the N -th symmetric product of the moduli space for the abelian case, even though a direct derivation is still evasive.

3. Brane tilings for M2 branes

In this work we restrict our attention to how brane tilings relate to M2-brane theories, although the relationship between tilings and the world-volume physics of D3-branes is a fascinating subject.

A brane tiling (or dimer model) is a periodic bipartite graph on the plane. Alternatively, we may draw it on the surface of a 2-torus by taking the smallest repeating structure (known as the fundamental domain) and identifying opposite edges [13]. The bipartite nature of the graph allows us to colour the nodes either white or black such that white nodes only connect to black nodes and vice versa.

There is a simple dictionary between a tiling and the Chern-Simons theory that it represents (Table 1). If a tiling is to correspond to a Chern-Simons theory, a set of levels, k_a must be specified. A tiling equipped with these levels is enough information to fully reconstruct a quiver Chern-Simons theory's Lagrangian [4, 8].

Tiling	Quiver	Meaning in gauge theory
Face (tile)	Node	$U(N)$ gauge group
Edge	Arrow	A bi-fundamental chiral multiplet
Node	A closed path*	An interaction term in the superpotential

Table 1. A brane tiling dictionary. *It is important to note that although each term of the superpotential corresponds to a closed path in the quiver, *not all* closed paths of the quiver give rise to the terms in the superpotential. White (black) nodes in the tiling correspond to positive (negative) superpotential terms.

The tiling and quiver of the well known ABJM model are given in Figure 1 as an illustrative example of how the two objects are related to one another.

3.1. From a brane tiling to the moduli space

The brane tiling is a very powerful tool for establishing the relationship between a large class of Chern-Simons theories and their mesonic moduli spaces. In this section we restrict ourselves to the study of abelian Chern-Simons theories corresponding to world-volume theories of one M2-brane.

When a quiver Chern-Simons theory admits a tiling description, we can easily construct the toric diagram of the mesonic moduli space by using the fast forward algorithm which is outlined below:

1. Assign an integer n_x to the edge corresponding to the chiral field X

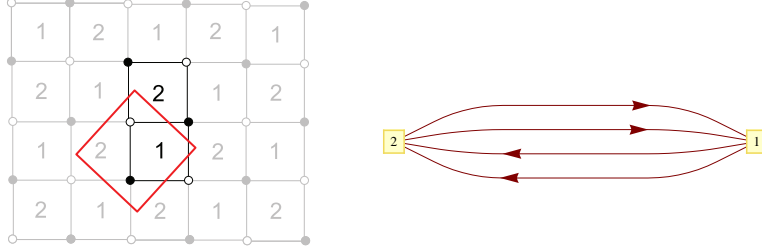


Fig. 1. An example of a brane tiling (left) and its corresponding quiver diagram (right). The red square in the tiling indicates the smallest unit of repetition called the *fundamental domain*. In (3+1) dimensions, this model is known as the conifold theory. In (2+1) dimensions, if a CS level k is assigned to one gauge group and $-k$ to the other, then the corresponding model is the ABJM theory.

(Figure 2) such that the CS level k_a of the gauge group a is given by²

$$k_a = \sum_{\text{all fields } X} d_{a_X} n_X, \quad (3.7)$$

where d_{a_X} is the charge of the chiral field X under the $U(1)$ gauge group a and can be read off from the quiver diagram easily. Due to the bipartite nature of the tiling, we see that the relation $\sum_a k_a = 0$ is automatically satisfied.

2. Define the *Kasteleyn matrix* $K(x, y, z)$ whose entries are given by

$$K_{pq}(x, y, z) = \sum_{X: p \leftrightarrow q} X z^{n_X} w_X(x, y), \quad (3.8)$$

where the summation runs over the edges corresponding to the chiral fields X connecting the node p and the node q , and the weight $w_X(x, y)$ takes the values $x^\alpha y^\beta$ (where α and β depend on the orientation of the edge) if the edge X crosses the fundamental domain and $w_X(x, y) = 1$ if it does not.

3. Take the permanent³ of the Kasteleyn matrix. It can be written in the form:

$$\text{perm } K = \sum_{\alpha=1}^c p_\alpha x^{u_\alpha} y^{v_\alpha} z^{w_\alpha}. \quad (3.9)$$

² This way of representing k_a is introduced in [4] and is also used in [28].

³ The permanent is similar to the determinant: the signatures of the permutations are not taken into account and all terms come with a + sign. One can also use the determinant but then certain signs must be introduced [13, 14].

Each p_α , which is a collection of the chiral fields, is called a *perfect matching*. It is known that the Master space is parametrised by the perfect matchings [27].

4. The coordinates $(u_\alpha, v_\alpha, w_\alpha)$ of the α -th point in the toric diagram are given respectively by the powers of x, y, z in (3.9). These coordinates can be collected in the columns of the following matrix:

$$G_K = \begin{pmatrix} u_1 & u_2 & u_3 & \dots & u_c \\ v_1 & v_2 & v_3 & \dots & v_c \\ w_1 & w_2 & w_3 & \dots & w_c \end{pmatrix}. \quad (3.10)$$

Remark 1: There are redundancies in the G_K matrix. In particular, we can construct \tilde{G}_K (a $(4 \times c)$ matrix) by prepending $(1 \ 1 \ 1 \ \dots \ 1)$ into the first row of the G_K matrix. After performing a series of elementary operations (or equivalently by applying a suitable $GL(4, \mathbb{Z})$ transformation) on the rows of \tilde{G}_K such that the first row is kept to be $(1 \ 1 \ 1 \ \dots \ 1)$, we then remove this first row and obtain another $3 \times c$ matrix G'_K . The matrices G_K and G'_K carry the same toric data, and hence correspond to the same mesonic moduli space⁴.

Remark 2: The G_K matrix contains information about the mesonic global symmetry of the theory. In particular, we can transform G_K as stated in Remark 1 so that the rows of the resulting matrix contain weights of the mesonic symmetry.

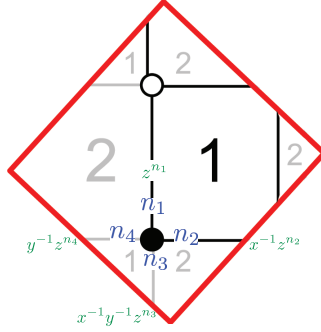


Fig. 2. The fundamental domain of the tiling of the ABJM theory. Assignments of the integers to the edges are shown in blue and the weights of these edges are shown in green.

⁴ This arbitrariness in how the fundamental domain was drawn on the tiling contributes to this redundancy.

4. Toric dualities

A toric duality is a situation in which one singular CY variety corresponds to more than one Chern-Simons theory (which we shall refer to as *toric phase*). Toric phases share several common features, even though their brane tilings are different:

- The mesonic moduli spaces of all phases are identical.
- The perfect matchings of different phases are exactly the same (including the labels and up to zero R-charge perfect matchings). They are charged in the same way under global symmetries.
- When written in terms of the perfect matchings, the mesonic generators of different phases are precisely the same (up to zero R-charge perfect matchings).

Let us now illustrate this idea of toric duality by giving different phases of the \mathbb{C}^4 theory as well as the $\mathcal{C} \times \mathbb{C}$ theory.

4.1. The \mathbb{C}^4 Theory

There are two known phases of the \mathbb{C}^4 theory:

Phase I: The ABJM theory with $\vec{k} = (1, -1)$. The quiver and tiling are drawn in Figure 1. In the abelian case ($N = 1$), the superpotential of the ABJM theory vanishes, as the chiral fields are simply complex numbers. Hence, the Master space is \mathbb{C}^4 . Since the number of gauge groups is $G = 2$, from (2.6), it follows that for the CS levels $\vec{k} = (1, -1)$ the mesonic moduli space is \mathbb{C}^4 . This is parametrised by X_{12}^i, X_{21}^i ($i = 1, 2$), each of which has an R-charge $1/2$.

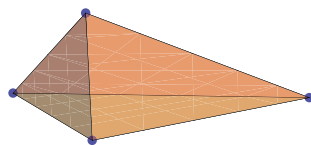


Fig. 3. The toric diagram of the \mathbb{C}^4 theory.

Phase II: The double bonded hexagon model with $\vec{k} = (1, -1)$. The quiver and tiling of this phase of \mathbb{C}^4 is drawn in Figure 4. By a similar argument to the one above, it can be shown that the mesonic moduli space for $\vec{k} = (1, -1)$ is also \mathbb{C}^4 [9]. This is parametrised by X_{12}, X_{21}, ϕ_i ($i = 1, 2$), each of which has an R-charge of $1/2$.

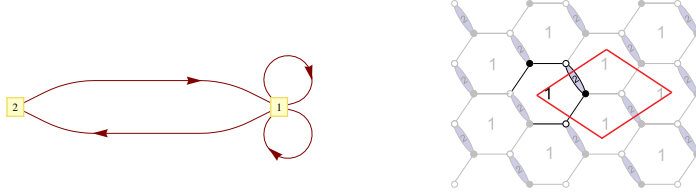


Fig. 4. Phase II of \mathbb{C}^4 . The superpotential is $W = \text{Tr}(X_{12}X_{21}[\phi_1, \phi_2])$.

4.2. The conifold $(\mathcal{C}) \times \mathbb{C}$ Theory

There are 3 known phases of the $\mathcal{C} \times \mathbb{C}$ theory. Their quivers and tilings are given in Figures 5, 6 and 7. The toric diagram is in Figure 8.

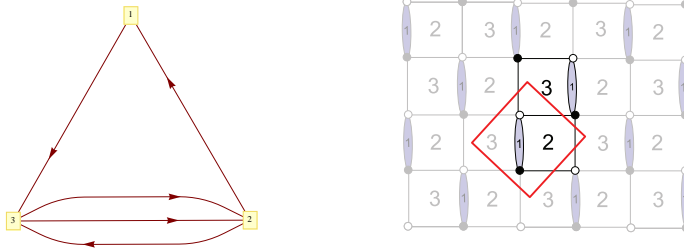


Fig. 5. Phase I of $\mathcal{C} \times \mathbb{C}$ with CS levels $k_1 = -k_2 = 1$, $k_3 = 0$

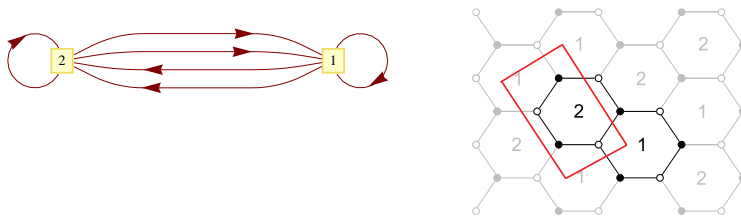


Fig. 6. Phase II of $\mathcal{C} \times \mathbb{C}$ with CS levels $k_1 = -k_2 = 1$

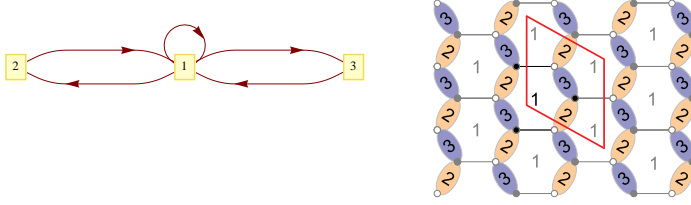


Fig. 7. Phase III of $\mathcal{C} \times \mathbb{C}$ with CS levels $k_1 = 0, k_2 = -k_3 = 1$

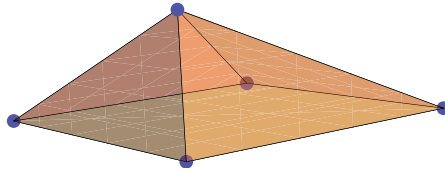


Fig. 8. The toric diagram of the $\mathcal{C} \times \mathbb{C}$ theory. The 4 points at the corners on the base form the toric diagram of the conifold (\mathcal{C}), and the point at the tip of the pyramid forms the toric diagram of \mathbb{C} .

4.2.1. A closer look at Phase II of $\mathcal{C} \times \mathbb{C}$

Let us focus on just one phase of the $\mathcal{C} \times \mathbb{C}$ theory. We summarise some of the interesting features of the model below:

- In (3+1) dimensions, the quiver and tiling correspond to the $\mathbb{C}^2/\mathbb{Z}_2 \times \mathbb{C}$ theory (Figure 6).
- Since the number of gauge groups is $G = 2$, it follows from (2.6) that the Master space is the same as the mesonic moduli space.
- From the superpotential

$$W = \text{Tr} (\phi_1 (X_{12}^2 X_{21}^1 - X_{12}^1 X_{21}^2) + \phi_2 (X_{21}^2 X_{12}^1 - X_{21}^1 X_{12}^2)) , \quad (4.11)$$

it can be shown [27] that the Master space (and hence the mesonic moduli space) is $\mathcal{C} \times \mathbb{C}$, where the conifold \mathcal{C} is parametrised by $X_{12}^1, X_{12}^2, X_{21}^1, X_{21}^2$ with the constraint $X_{12}^1 X_{21}^2 = X_{12}^2 X_{21}^1$, and the \mathbb{C} is parametrised by $\phi_1 = \phi_2$.

- It follows that ϕ_1, ϕ_2 are free fields, and so each of them has an R-charge of $1/2$. By symmetry, it can be seen that the requirement of R-charge 2 to W divides $3/2$ equally among two X fields. Hence, each of the X fields carries an R-charge of $3/4$.

- Chiral fields have non-trivial scaling dimensions. Hence, the IR fixed point is non-trivial.
- The R-charges derived above agree with the computation by minimising the volume of the corresponding SE manifold [8, 9]. This provides a (weak) test of the AdS/CFT correspondence.

4.2.2. The global symmetry and charges

The global symmetry of the $\mathcal{C} \times \mathbb{C}$ theory is $SU(2) \times SU(2) \times U(1)_q \times U(1)_R \times U(1)_B$. The charges of the perfect matchings under the global symmetry are given in Table 2. The mesonic generators of each phase are listed in Table 3. The mesonic Hilbert series of $\mathcal{C} \times \mathbb{C}$ is

$$\begin{aligned}
 g_1^{\text{mes}}(t_1, t_2, x_1, x_2) &= \frac{1}{1-t_2} \times \frac{1-t_1^4}{(1-t_1^2 x_1 x_2) \left(1 - \frac{t_1^2 x_2}{x_1}\right) \left(1 - \frac{t_1^2 x_1}{x_2}\right) \left(1 - \frac{t_1^2}{x_1 x_2}\right)} \\
 &= \sum_{i=0}^{\infty} t_2^i \sum_{n=0}^{\infty} [n; n] t_1^{2n} , \tag{4.12}
 \end{aligned}$$

where $t_1 = t^3 q$ and $t_2 = t^4/q^4$. Note that the first factor is the Hilbert series of \mathbb{C} and the second factor is the Hilbert series of \mathcal{C} .

	$SU(2)_1$	$SU(2)_2$	$U(1)_q$	$U(1)_B$	$U(1)_R$	fugacity
p_1	1	0	1	1	3/8	$t^3 q b x_1$
p_2	-1	0	1	1	3/8	$t^3 q b/x_1$
p_3	0	1	1	-1	3/8	$t^3 q x_2/b$
p_4	0	-1	1	-1	3/8	$t^3 q/(b x_2)$
p_5	0	0	-4	0	1/2	t^4/q^4

Table 2. The global symmetry of the $\mathcal{C} \times \mathbb{C}$ theory. Here t is the chemical potential (or strictly speaking the fugacity) associated with the $U(1)_R$ charges. The power of t counts R-charges in units of 1/8, q is the fugacity associated with the $U(1)_q$ charges, and x_1, x_2 are respectively the $SU(2)_1, SU(2)_2$ weights.

5. M2-brane theories and Fano 3-folds

In this section, we focus on gauge theories arising from M2-branes probing CY 4-fold singularities that can be realised as cones over smooth toric Fano 3-folds. These Fano varieties have already attracted much mathematical interest and a complete classification of these geometries is known [29]. There are precisely 18 smooth toric Fano 3-folds [21, 22]. In this paper,

Perfect Matchings	Generators of Phase I	Generators of Phase II	Generators of Phase III
$p_1 p_3$	$X_{13} X_{32}^1$	X_{12}^1	$X_{21} X_{12}$
$p_2 p_3$	$X_{13} X_{32}^2$	X_{21}^1	$X_{21} X_{13}$
$p_1 p_4$	$X_{23} X_{32}^1$	X_{12}^2	$X_{31} X_{12}$
$p_2 p_4$	$X_{23} X_{32}^2$	X_{21}^2	$X_{21} X_{13}$
p_5	X_{21}	$\phi_1 = \phi_2$	ϕ_1

Table 3. A comparison between the generators of different phases of the $\mathcal{C} \times \mathcal{C}$ theory. In terms of the perfect matchings, the generators of different phases are precisely the same.

we present the gauge theories corresponding to 5 of them, namely $\mathbb{P}^2 \times \mathbb{P}^1$, $\mathbb{P}^1 \times \mathbb{P}^1 \times \mathbb{P}^1$, $dP_n \times \mathbb{P}^1$ ($n = 1, 2, 3$). For more information about the others, we refer the reader to [20] and the work in progress [31].

5.1. The $M^{1,1,1}$ Theory

The quiver and tiling are given in Figure 9. In $(3 + 1)$ dimensions, this corresponds to the dP_0 theory. Let us assign the CS levels $\vec{k} = (1, -2, 1)$. The superpotential is $W = \text{Tr} \left(\epsilon_{ijk} X_{12}^i X_{23}^j X_{31}^k \right)$.

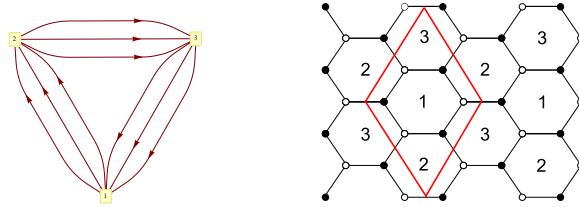


Fig. 9. (i) Quiver diagram of the $M^{1,1,1}$ theory. (ii) Tiling of the $M^{1,1,1}$ theory.

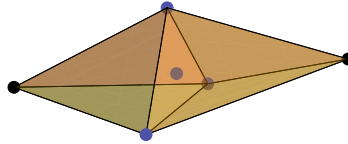


Fig. 10. The toric diagram of the $M^{1,1,1}$ theory.

The toric diagram of this theory is given by Figure 10. Note that the 4 blue points form the toric diagram of \mathbb{P}^2 , and the 2 black points together

with the blue internal point form the toric diagram of \mathbb{P}^1 . Hence, this theory corresponds to the cone over $\mathbb{P}^2 \times \mathbb{P}^1$.

The mesonic global symmetry of this theory is $SU(3) \times SU(2) \times U(1)_R$. There is also one baryonic $U(1)_B$ symmetry. The charges of the perfect matchings under these symmetries are listed in Table 4. The Hilbert series of the mesonic moduli space is given by

$$g^{\text{mes}}(t, x, y_1, y_2; M^{1,1,1}) = \sum_{n=0}^{\infty} [3n, 0; 2n] t^{18n} . \quad (5.13)$$

This is a sum over all irreducible representations of the form $[3n, 0; 2n]$, where the first two numbers are highest weights of an $SU(3)$ representation (totally symmetric $3n$ tensor), and the last number is the highest weight of an $SU(2)$ representation (of spin n). Indeed, this result confirms the known KK spectrum on $M^{1,1,1}$ [30].

	$SU(3)$	$SU(2)$	$U(1)_R$	$U(1)_B$	fugacity
p_1	(1, 0)	0	4/9	0	$t^4 y_1$
p_2	(-1, 1)	0	4/9	0	$t^4 y_2 / y_1$
p_3	(0, -1)	0	4/9	0	t^4 / y_2
r_1	(0, 0)	1	1/3	-1	$t^3 x / b$
r_2	(0, 0)	-1	1/3	-1	$t^3 / (xb)$
s_1	(0, 0)	0	0	2	b^2

Table 4. Charges of the perfect matchings under the global symmetry of the $M^{1,1,1}$ theory. Here t is the fugacity of the R-charge (in multiples of $1/9$), y_1, y_2 are the fugacities of the $SU(3)$ symmetry, x is the fugacity of the $SU(2)$ symmetry and b is the fugacity of the $U(1)_B$ symmetry. We have used the notation (a, b) to represent a weight of $SU(3)$.

5.2. The $Q^{1,1,1}/\mathbb{Z}_2$ Theory

There are two known toric phases of this theory. Their quivers and tilings are given in Figures 11 and 12. The toric diagram is drawn in Figure 13. This theory corresponds to the cone over $\mathbb{P}^1 \times \mathbb{P}^1 \times \mathbb{P}^1$.

The mesonic symmetry of this model is $SU(2)^3 \times U(1)_R$. There are two baryonic charges. The charges of perfect matchings under these symmetries are given in Table 5. The Hilbert series of the mesonic moduli space can be written as

$$g_1^{\text{mes}}(t, x_1, x_2, x_3; Q^{1,1,1}/\mathbb{Z}_2) = \sum_{n=0}^{\infty} [2n; 2n; 2n] t^{6n} . \quad (5.14)$$



Fig. 11. The quiver and tiling of Phase I of $Q^{1,1,1}/\mathbb{Z}_2$ with $\vec{k} = (1, -1, -1, 1)$. The superpotential is $W = \epsilon_{ij\epsilon_{pq}} \text{Tr}(X_{12}^i X_{23}^p X_{34}^j X_{41}^q)$.

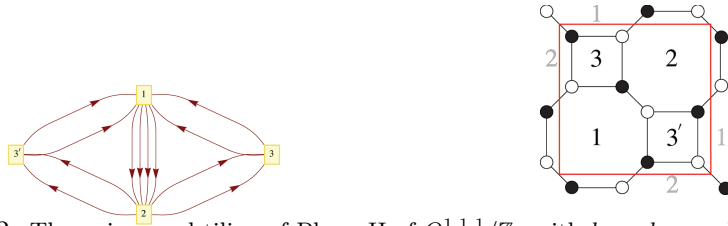


Fig. 12. The quiver and tiling of Phase II of $Q^{1,1,1}/\mathbb{Z}_2$ with $k_1 = k_2 = -k_3 = -k_{3'} = 1$. The superpotential is $W = \epsilon_{ij\epsilon_{kl}} \text{Tr}(X_{12}^{ik} X_{23}^l X_{31}^j) - \epsilon_{ij\epsilon_{kl}} \text{Tr}(X_{12}^{ki} X_{23'}^l X_{3'1}^j)$.

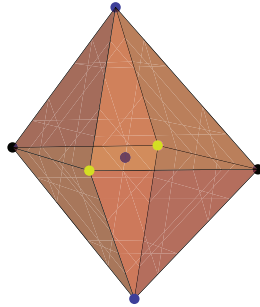


Fig. 13. The toric diagram of $Q^{1,1,1}/\mathbb{Z}_2$. Note that the 3 blue points form the toric diagram of \mathbb{P}^1 , and so as the yellow points (together with the internal points) and the black points (together with the internal point). Thus, this theory corresponds to the cone over $\mathbb{P}^1 \times \mathbb{P}^1 \times \mathbb{P}^1$.

5.3. The $dP_n \times \mathbb{P}^1$ Theories

Tilings have been found that correspond to the cones over $dP_n \times \mathbb{P}^1$, for $1 \leq n \leq 3$. We present both the quiver diagrams and tilings Figures 14, 15, 16 and their corresponding toric data Figure 17. Full details of these models will be presented in future work [31].

	$SU(2)_1$	$SU(2)_2$	$SU(2)_3$	$U(1)_R$	$U(1)_{B_1}$	$U(1)_{B_2}$	fugacity
p_1	1	0	0	1/3	1	0	tb_1x_1
p_2	-1	0	0	1/3	1	0	tb_1/x_1
q_1	0	1	0	1/3	0	0	tx_2
q_2	0	-1	0	1/3	0	0	t/x_2
r_1	0	0	1	1/3	-1	-1	$tx_3/(b_1b_2)$
r_2	0	0	-1	1/3	-1	-1	$t/(x_3b_1b_2)$
s_1	0	0	0	0	0	2	b_2^2
s_2	0	0	0	0	0	0	1
s_3	0	0	0	0	0	0	1

Table 5. The global symmetry of the $Q^{1,1,1}/\mathbb{Z}_2$ theory. Here t is the fugacity of R-charge, x_1, x_2, x_3 are weights of $SU(2)_1, SU(2)_2, SU(2)_3$, and b_1, b_2 are baryonic fugacities of $U(1)_{B_1}, U(1)_{B_2}$. Note that the perfect matching s_3 does not exist in Phase I but exists in Phase II.

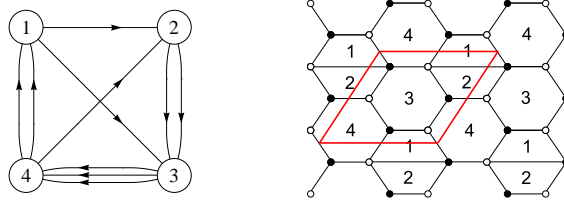


Fig. 14. [The $dP_1 \times \mathbb{P}^1$ theory] (i) Quiver diagram (ii) Tiling. The Chern-Simons levels are $\vec{k} = (1, 1, -1, -1)$. The superpotential is $W = \text{Tr} [\epsilon_{ij} (X_{13}X_{34}^iX_{41}^j + X_{42}X_{23}^iX_{34}^j + X_{12}X_{23}^jX_{34}^3X_{41}^i)]$.

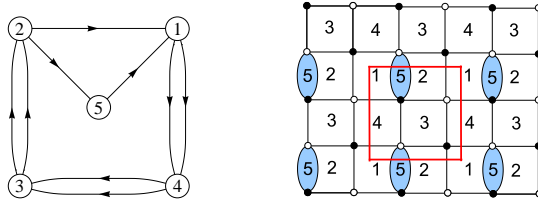


Fig. 15. [The $dP_2 \times \mathbb{P}^1$ theory] (i) Quiver diagram (ii) Tiling. The Chern-Simons levels are $\vec{k} = (1, 1, -1, 0, -1)$. The superpotential is $W = \text{Tr} [\epsilon_{ij} (X_{43}^1X_{32}^jX_{21}X_{14}^i + X_{51}X_{14}^jX_{43}^2X_{32}^iX_{25})]$.

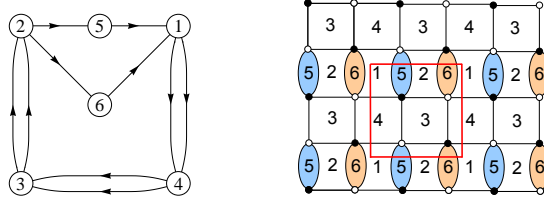


Fig. 16. [The $dP_3 \times \mathbb{P}^1$ theory] (i) Quiver diagram (ii) Tiling. The Chern-Simons levels are $\vec{k} = (0, -1, 0, -1, 1, 1)$. The superpotential is $W = \text{Tr} [\epsilon_{ij} (X_{14}^j X_{43}^2 X_{32}^i X_{26} X_{61} + X_{14}^i X_{43}^1 X_{32}^j X_{25} X_{51})]$.

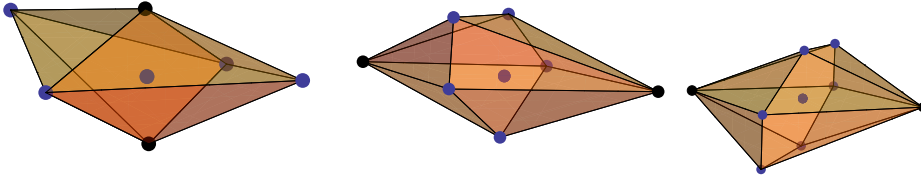


Fig. 17. The toric diagrams of (i) left: the $dP_1 \times \mathbb{P}^1$ theory, (ii) middle: the $dP_2 \times \mathbb{P}^1$ theory, (ii) right: the $dP_3 \times \mathbb{P}^1$ theory. In each figure, the blue points form the toric diagram of dP_n and the black points (together with the blue internal point) form a toric diagram of \mathbb{P}^1 .

REFERENCES

- [1] B. S. Acharya, J. M. Figueroa-O'Farrill, C. M. Hull and B. J. Spence, Adv. Theor. Math. Phys. **2** (1999) 1249 [arXiv:hep-th/9808014].
- [2] D. R. Morrison and M. R. Plesser, Adv. Theor. Math. Phys. **3** (1999) 1 [arXiv:hep-th/9810201].
- [3] D. Martelli and J. Sparks, arXiv:0808.0912 [hep-th].
- [4] A. Hanany and A. Zaffaroni, arXiv:0808.1244 [hep-th].
- [5] K. Ueda and M. Yamazaki, arXiv:0808.3768 [hep-th].
- [6] A. Hanany and Y. H. He, arXiv:0811.4044 [hep-th].
- [7] J. Hewlett and Y. H. He, arXiv:0909.2879 [hep-th].
- [8] A. Hanany, D. Vegh, A. Zaffaroni, arXiv:0809.1440.
- [9] J. Davey, A. Hanany, N. Mekareeya and G. Torri, arXiv:0903.3234 [hep-th].
- [10] J. Davey, A. Hanany, N. Mekareeya and G. Torri, arXiv:0908.4033 [hep-th].
- [11] N. Benishiti, Y. H. He and J. Sparks, arXiv:0909.4557 [hep-th].
- [12] J. Davey, A. Hanany and J. Pasukonis, arXiv:0909.2868 [hep-th].
- [13] A. Hanany and K. D. Kennaway, hep-th/0503149.
- [14] S. Franco, A. Hanany, K. D. Kennaway, D. Vegh and B. Wecht, JHEP **0601**, 096 (2006) [arXiv:hep-th/0504110].

- [15] A. Hanany and D. Vegh, JHEP **0710**, 029 (2007) [arXiv:hep-th/0511063].
- [16] S. Franco, A. Hanany, D. Martelli, J. Sparks, D. Vegh and B. Wecht, JHEP **0601**, 128 (2006) [arXiv:hep-th/0505211].
- [17] K. D. Kennaway, Int. J. Mod. Phys. A **22**, 2977 (2007) [arXiv:0706.1660 [hep-th]].
- [18] M. Yamazaki, Fortsch. Phys. **56**, 555 (2008) [arXiv:0803.4474 [hep-th]].
- [19] A. Amariti, D. Forcella, L. Girardello and A. Mariotti, arXiv:0903.3222 [hep-th].
- [20] A. Hanany and Y. H. He, arXiv:0904.1847 [hep-th].
- [21] V. V. Batyrev, Math. USSR-Izv. 19, 13-25 (1982)
- [22] <http://malham.kent.ac.uk/grdb/index.php>
- [23] B. Feng, A. Hanany and Y. H. He, Nucl. Phys. B **595**, 165 (2001) [arXiv:hep-th/0003085].
- [24] B. Feng, A. Hanany and Y. H. He, JHEP **0108**, 040 (2001) [arXiv:hep-th/0104259].
- [25] B. Feng, S. Franco, A. Hanany and Y. H. He, JHEP **0308** (2003) 058 [arXiv:hep-th/0209228].
- [26] B. Feng, S. Franco, A. Hanany and Y. H. He, JHEP **0212**, 076 (2002) [arXiv:hep-th/0205144].
- [27] D. Forcella, A. Hanany, Y. H. He and A. Zaffaroni, JHEP **0808**, 012 (2008) [arXiv:0801.1585 [hep-th]]; Lett. Math. Phys. **85**, 163 (2008) [arXiv:0801.3477 [hep-th]]. D. Forcella, arXiv:0902.2109 [hep-th].
- [28] Y. Imamura and K. Kimura, arXiv:0808.4155 [hep-th].
- [29] S. Mori, S. Mukai, Papers from the symposium dedicated to the memory of Dr. Takehiko Miyata held in Kinosaki, October 30-November 9, 1984. Tokyo: Kinokuniya Company Ltd. 496-545 (1986)
J.-P. Murre, Proc. 2nd 1981 Sess. C.I.M.E., Varenna/Italy 1981, Lect. Notes Math. 947, 35-92 (1982).
S. D. Cutkosky, Manuscr. Math. 64, No.2, 189-204 (1989).
- [30] D. Fabbri, P. Fre', L. Gualtieri, C. Reina, A. Tomasiello, A. Zaffaroni and A. Zampa, Nucl. Phys. B **577**, 547 (2000) [arXiv:hep-th/9907219].
- [31] J. Davey, et al., "M2-Branes and Fano 3-folds". To appear